

Gravitational wave signal from massive gravity

A. Emir Gümrükçüoğlu,^{1,*} Sachiko Kuroyanagi,^{2,†}
 Chunshan Lin,^{1,‡} Shinji Mukohyama,^{1,§} and Norihiro Tanahashi^{3,¶}

¹*Kavli Institute for the Physics and Mathematics of the Universe,
 Todai Institutes for Advanced Study, University of Tokyo,
 5-1-5 Kashiwanoha, Kashiwa, Chiba 277-8583, Japan*

²*Research Center for the Early Universe (RESCEU),
 Graduate School of Science, The University of Tokyo, Tokyo 113-0033, Japan*
³*Department of Physics, University of California, Davis, CA 95616, USA*

(Dated: August 30, 2012)

We discuss the detectability of gravitational waves with a time dependent mass contribution, by means of the stochastic gravitational wave observations. Such a mass term typically arises in the cosmological solutions of massive gravity theories. We conduct the analysis based on a general quadratic action, and thus the results apply universally to any massive gravity theories in which modification of general relativity appears primarily in the tensor modes. The primary manifestation of the modification in the gravitational wave spectrum is a sharp peak. The position and height of the peak carry information on the present value of the mass term, as well as the duration of the inflationary stage. We also discuss the detectability of such a gravitational wave signal using the future-planned gravitational wave observatories.

PACS numbers:

I. INTRODUCTION

Since the pioneering model of massive gravity was proposed by Fierz and Pauli [1], numerous attempts have been made to introduce a non-zero mass to graviton. This issue has been attracting a great deal of interest, partly because graviton mass may provide an alternative explanation for the acceleration of our universe. Namely, instead of attributing it to the existence of dark energy whose origin is still unknown, the acceleration may be simply due to modification of gravity.

Until recently, however, it has been thought that such modification by non-zero graviton mass is extremely difficult, typically leading to the emergence of ghost degrees of freedom and various pathologies. As first shown by Boulware and Deser [2], the source of these difficulties is associated with a helicity-0 mode in the gravity sector, which is absent at the quadratic order of the Fierz-Pauli massive gravity but revives at the higher order and acts as a ghost, dubbed the *Boulware-Deser (BD) ghost*. A remedy for this difficulty was recently proposed by Refs. [3, 4], in which the would-be BD ghost is eliminated by adding higher-order correction terms order by order and by resumming them into a three parameter expression. Non-existence of the BD ghost in this theory was discussed and proved in Refs. [5–11]. Various solutions in the theory were studied in Refs. [12–26]. Therefore this nonlinear theory of massive gravity can be considered as a nonlinear completion of the Fierz-Pauli theory, which is the simplest and the oldest linear massive gravity theory. Having this in mind, we consider it quite natural to suppose that other massive gravity theories or, more generally, Higgs phases of gravity might find their nonlinear completions in the future.

Such examples include, but are not restricted to, ghost condensate [27, 28] and Lorentz-violating massive gravity theories [29, 30]. In these examples, propagating degrees of freedom do not form a representation of 4-dimensional Poincaré symmetry even in the exact Minkowski background. Instead, they form representations of 3-dimensional rotational and translational symmetries. As a result, physical degrees of freedom are classified into scalar, vector and tensor parts, according to their transformation properties under the 3-dimensional spatial rotation. Modes in different classes may behave rather differently. For instance, in the case of ghost condensate in Minkowski background, propagating degrees of freedom in the gravity sector are two tensor modes and one scalar mode. The two tensor modes

*Electronic address: emir.gumrukcuoglu@ipmu.jp

†Electronic address: skuro@resceu.s.u-tokyo.ac.jp

‡Electronic address: chunshan.lin@ipmu.jp

§Electronic address: shinji.mukohyama@ipmu.jp

¶Electronic address: tanahashi@ms.physics.ucdavis.edu

behave exactly like those in general relativity (GR) while the scalar mode has an unusual dispersion relation, i.e. non-relativistic dispersion relation without a mass gap. On the other hand, in a particular class of models among those proposed in [30], propagating degrees of freedom in the gravity sector are two tensor modes only, and their dispersion relation is massive and relativistic. From the point of view of the symmetry, i.e. 3-dimensional spatial rotational symmetry, we expect that there should be even wider classes of models in which scalar, vector, and tensor parts behave differently.

In the present paper, for definiteness we mainly focus on a class of massive gravity models in which propagating degrees of freedom in gravity sector are only two tensor modes with a massive dispersion relation. In this case, the scalar and vector sectors behave exactly like in GR and the only modification emerges in the tensor sector: the dispersion relation of gravitational waves acquires an effective mass, which in general can be time-dependent. We shall discuss an attempt towards a nonlinear completion of such massive gravity models, but in most part of the present paper we shall consider this class of models as a purely phenomenological one to be constrained or probed by observations and experiments. We conduct the analysis based on a general quadratic action for tensor modes, and thus our results apply not only to the theories with precisely two propagating gravitational modes but also to a more general class of theories in which modification of gravity appears primarily in the tensor modes.

Being different from GR only in the tensor sector, observation of gravitational waves and/or their imprints would be the most efficient probe for the model. Therefore, in this paper we address the detectability of the effective mass of gravitational waves by means of the stochastic gravitational wave observations.

The rest of this paper is organized as follows. After describing our model in Sec. II, we discuss an attempt towards nonlinear completion of the model in Sec. III. This consideration at the very least shows that the structure of the model considered in the present paper is not forbidden by the symmetry. However, readers who are interested only in purely phenomenological aspects can safely skip Sec. III. We then derive analytic formulas for the power-spectrum of stochastic gravitational waves and discuss how to read off information about the effective mass of gravitational waves in Sec. IV. In Sec. V we show some numerical results and make comparison with the analytical results of the previous section. Sec. VI is devoted to a summary of the results and discussions.

II. MODEL DESCRIPTION

In the present paper we shall consider linear massive gravity models that respect the symmetry of Friedmann-Robertson-Walker (FRW) universe, i.e. the spatial homogeneity and isotropy. Metric perturbations are thus decomposed into scalar, vector and tensor parts, according to the transformation properties under the 3-dimensional spatial rotation.

We restrict our considerations to a class of models in which propagating degrees of freedom in the gravity sector are two tensor modes only. For tensor-type perturbations on the FRW background, the metric can be written as

$$g_{\mu\nu}dx^\mu dx^\nu = -N(t)^2 dt^2 + a(t)^2 [\Omega_{ij}(x^k) + \gamma_{ij}] dx^i dx^j, \quad \Omega_{ij}(x^k) = \delta_{ij} + \frac{K\delta_{il}\delta_{jm}x^l x^m}{1 - K\delta_{lm}x^l x^m}. \quad (1)$$

where γ_{ij} is the tensor-type perturbations satisfying

$$D^i \gamma_{ij} = 0, \quad \Omega^{ij} \gamma_{ij} = 0. \quad (2)$$

Here, $\Omega^{ij} = (\Omega^{-1})^{ij}$, $D^i = \Omega^{ij} D_j$ and D_j is the spatial covariant derivative compatible with the metric Ω_{ij} .

By assumption, the quadratic action for the perturbation should be invariant under the spatial rotation and translation. Hence we can use the following ingredients to construct the quadratic action describing the dynamics of the tensor perturbation:

$$Ndt, \quad \sqrt{\Omega} d^3 \vec{x}, \quad \Omega_{ij}, \quad D_i, \quad \gamma_{ij}, \quad \frac{1}{N} \dot{\gamma}_{ij}, \quad (3)$$

provided that spatial indices are properly contracted to form scalar quantities. Here, $\Omega \equiv \det \Omega_{ij}$ and an overdot represents derivative with respect to the time coordinate t . Since the time coordinate t is invariant under the spatial rotation and translation, we can also use general functions of t and their derivatives.

We also demand that the action should include only up to second time derivatives of γ_{ij} in order to avoid ghosts in the linear level and that the system respects the spatial parity invariance.

Thus, after integration by parts, one can show that the general quadratic action is of the form

$$I_{tensor}^{(2)} = \frac{M_{Pl}^2}{8} \int dt d^3 x N a^3 \sqrt{\Omega} F(t) \left[\frac{1}{N^2} \dot{\gamma}^{ij} \dot{\gamma}_{ij} + \gamma^{ij} \left(\sum_{n=0}^{\infty} c_n(t) \frac{\Delta^n}{a^{2n}} \right) \gamma_{ij} \right], \quad (4)$$

where $\gamma^{ij} \equiv \Omega^{ik}\Omega^{jl}\gamma_{kl}$, $\Delta \equiv D^i D_i$ is the Laplacian operator associated with Ω_{ij} , $F(t)$ and $c_n(t)$ ($n = 0, 1, \dots$) are general functions of the time coordinate t . Note that $F(t)$ must be positive definite in order to avoid appearance of ghost and strong coupling. We can then set $F(t) = 1$ by a field redefinition, to be more precise, by a conformal transformation. Finally, in order to describe low energy phenomena such as cosmological evolution of gravitational waves at late time, we truncate the series expansion (the sum over n) at the second order spatial derivatives and obtain

$$I_{tensor}^{(2)} = \frac{M_{Pl}^2}{8} \int dt d^3x N a^3 \sqrt{\Omega} \left[\frac{1}{N^2} \dot{\gamma}^{ij} \dot{\gamma}_{ij} + \frac{c_g^2(t)}{a^2} \gamma^{ij} (\Delta - 2K) \gamma_{ij} - M_{GW}^2(t) \gamma^{ij} \gamma_{ij} \right], \quad (5)$$

where we have set $F = 1$ by a field redefinition (or a conformal transformation) and we have defined

$$c_g^2(t) \equiv c_1(t), \quad M_{GW}^2(t) \equiv -c_0(t) - \frac{2Kc_1(t)}{a^2}. \quad (6)$$

Note that physical meaning of c_g and M_{GW} are the sound speed and effective mass of gravitational waves.

Taking advantages of the background symmetry, it is convenient to expand γ_{ij} as

$$\gamma_{ij} = \sum_{\lambda} \int k^2 dk \gamma_{k,\lambda} Y_{ij}^{\lambda}(\vec{k}, \vec{x}), \quad (7)$$

where $k^2 \equiv \Omega_{ij} \vec{k}^i \vec{k}^j$, λ denotes the helicity state and Y_{ij}^{λ} is the tensor harmonics satisfying

$$(\Delta + k^2) Y_{ij}^{\lambda} = 0, \quad D^i Y_{ij}^{\lambda} = 0, \quad \Omega^{ij} Y_{ij}^{\lambda} = 0, \quad \int d^3x \sqrt{\Omega} \Omega^{ij} \Omega^{kl} Y_{ik}^{\lambda}(\vec{k}, \vec{x}) Y_{jl}^{\lambda'}(\vec{k}', \vec{x}) = 32\pi^2 \delta_{\lambda\lambda'} \delta^3(\vec{k} + \vec{k}'). \quad (8)$$

The equation of motion for $\gamma_{k,\lambda}$ is then

$$\bar{\gamma}_k'' + \left(c_g^2 k^2 + a^2 M_{GW}^2 - \frac{a''}{a} + 2Kc_g^2 \right) \bar{\gamma}_k = 0, \quad \bar{\gamma}_k \equiv a \gamma_k, \quad (9)$$

where the prime ($'$) denotes derivative with respect to the conformal time η defined by $d\eta \equiv N dt/a$. Since the equation of motion is identical for both polarizations, we omit the index λ hereafter.

III. AN ATTEMPT TOWARD NONLINEAR COMPLETION

The nonlinear theory of massive gravity recently proposed by Refs. [3, 4] eliminates the renowned BD ghost by construction and thus can be considered as a nonlinear completion of the Fierz-Pauli theory, which is the simplest and the oldest among all linear massive gravity theories. Having this in mind, we consider it quite possible that the phenomenological model described in the previous section might also find its nonlinear completions in the future.

In this section we discuss an attempt towards such a nonlinear completion. In particular, we shall derive the model with $c_g = 1$ precisely, based on a non-trivial background in the nonlinear theory of massive gravity. Unfortunately, this construction is purely classical and fails at the quantum level [31].¹ Nonetheless, at the very least it shows that the structure of the model considered in the present paper, with $c_g = 1$, is not forbidden by symmetry. Readers who are interested only in purely phenomenological aspects can safely skip this section.

The covariant action of the nonlinear massive gravity is constructed out of a 4-dimensional metric $g_{\mu\nu}$ and four scalar fields φ^a ($a = 0, 1, 2, 3$) called *Stückelberg fields*. The Stückelberg fields enter the action only through the tensor $f_{\mu\nu}$ defined as

$$f_{\mu\nu} = \bar{f}_{ab}(\varphi^c) \partial_{\mu} \varphi^a \partial_{\nu} \varphi^b, \quad (10)$$

where $\bar{f}_{ab}(\varphi^c)$ is a non-degenerate, second-rank symmetric tensor in the field space. The spacetime metric $g_{\mu\nu}$ and the tensor $f_{\mu\nu}$ are often called *physical metric* and *fiducial metric*, respectively.

¹ Adopting a different approach, Ref. [32] achieved a similar conclusion.

The gravity action is the sum of the Einstein-Hilbert action $I_{EH,\Lambda}$ (including a bare cosmological constant Λ) and the graviton mass term I_{mass} specified below. Adding the matter action I_{matter} , the total action is

$$I = I_{EH,\Lambda}[g_{\mu\nu}] + I_{mass}[g_{\mu\nu}, f_{\mu\nu}] + I_{matter}[g_{\mu\nu}, \sigma_I], \quad (11)$$

where

$$I_{EH,\Lambda}[g_{\mu\nu}] = \frac{M_{Pl}^2}{2} \int d^4x \sqrt{-g} (R - 2\Lambda), \quad (12)$$

$$I_{mass}[g_{\mu\nu}, f_{\mu\nu}] = M_{Pl}^2 m_g^2 \int d^4x \sqrt{-g} (\mathcal{L}_2 + \alpha_3 \mathcal{L}_3 + \alpha_4 \mathcal{L}_4), \quad (13)$$

and $\{\sigma_I\}$ ($I = 1, 2, \dots$) represent generic matter fields. Each contribution in the mass term I_{mass} is constructed as

$$\begin{aligned} \mathcal{L}_2 &= \frac{1}{2} ([\mathcal{K}]^2 - [\mathcal{K}^2]), \\ \mathcal{L}_3 &= \frac{1}{6} ([\mathcal{K}]^3 - 3 [\mathcal{K}] [\mathcal{K}^2] + 2 [\mathcal{K}^3]), \\ \mathcal{L}_4 &= \frac{1}{24} ([\mathcal{K}]^4 - 6 [\mathcal{K}]^2 [\mathcal{K}^2] + 3 [\mathcal{K}^2]^2 + 8 [\mathcal{K}] [\mathcal{K}^3] - 6 [\mathcal{K}^4]), \end{aligned} \quad (14)$$

where the square brackets denote trace operation and

$$\mathcal{K}_\nu^\mu = \delta_\nu^\mu - \left(\sqrt{g^{-1}f} \right)_\nu^\mu. \quad (15)$$

The square-root in this expression is the positive definite matrix defined through

$$\left(\sqrt{g^{-1}f} \right)_\rho^\mu \left(\sqrt{g^{-1}f} \right)_\nu^\rho = f_\nu^\mu \equiv g^{\mu\rho} f_{\rho\nu}. \quad (16)$$

Note that the fiducial metric is not dynamical but fixed by the theory. In other words, the form of the fiducial metric is a part of definition of the theory. Of course, an apparent form of the fiducial metric is subject to changes under redefinition and dynamics of the Stückelberg fields. However, such changes are equivalent to coordinate transformations of the metric in the field space and thus do not change geometrical properties such as the curvature tensor in the field space. For example, if we demand the maximal symmetry, i.e. Poincaré, de Sitter or anti-de Sitter symmetry, in the field space then the fiducial metric must be Minkowski, de Sitter or anti-de Sitter metric, respectively, regardless of appearances.

In the present paper we consider a general fiducial metric of the FRW type, specified by the lapse function $n(\varphi^0)$, the scale factor $\alpha(\varphi^0)$ and the spacial curvature constant K :

$$f_{\mu\nu} = -n^2(\varphi^0) \partial_\mu \varphi^0 \partial_\nu \varphi^0 + \alpha^2(\varphi^0) \Omega_{ij}(\varphi^k) \partial_\mu \varphi^i \partial_\nu \varphi^j, \quad \Omega_{ij}(\varphi^k) = \delta_{ij} + \frac{K \delta_{il} \delta_{jm} \varphi^l \varphi^m}{1 - K \delta_{lm} \varphi^l \varphi^m}. \quad (17)$$

Needless to say, this class of fiducial metrics include Minkowski, de Sitter and anti-de Sitter fiducial metrics as special cases. For example, a Minkowski fiducial metric can be rewritten as an open FRW form and allows non-trivial cosmology [18]. Note, however, that the Minkowski fiducial metric does not allow flat nor closed FRW cosmology [17]. Similarly, an anti-de Sitter fiducial metric allows non-trivial open FRW cosmology but does not allow flat nor closed ones (see Appendix B). On the other hand, non-trivial open, flat, closed FRW cosmologies can be realized with a de Sitter fiducial metric (see Appendix B, and see also Ref. [33, 34] for related discussions).

In this section we consider a general FRW background plus perturbations.

$$g_{\mu\nu} = g_{\mu\nu}^{(0)} + \delta g_{\mu\nu}, \quad \varphi^a = x^a + \pi^a + \frac{1}{2} \pi^b \partial_b \pi^a + O(\epsilon^3), \quad (18)$$

where

$$g_{\mu\nu}^{(0)} dx^\mu dx^\nu = -N(t)^2 dt^2 + a(t)^2 \Omega_{ij}(x^k) dx^i dx^j, \quad \Omega_{ij}(x^k) = \delta_{ij} + \frac{K \delta_{il} \delta_{jm} x^l x^m}{1 - K \delta_{lm} x^l x^m}. \quad (19)$$

Here, the perturbation π^a of the Stückelberg fields was defined through the exponential map, following [33]. The background equations of motion lead to

$$3H^2 + \frac{3K}{a^2} = \Lambda_\pm + \frac{1}{M_{Pl}^2} \rho, \quad -\frac{2\dot{H}}{N} + \frac{2K}{a^2} = \frac{1}{M_{Pl}^2} (\rho + P), \quad \frac{\alpha(t)}{a(t)} = X_\pm, \quad (20)$$

where a dot represents derivative with respect to t , $H \equiv \dot{a}/(Na)$ is the Hubble expansion rate of the background physical metric, ρ and P are the matter energy density and pressure, and

$$X_{\pm} \equiv \frac{1 + 2\alpha_3 + \alpha_4 \pm \sqrt{1 + \alpha_3 + \alpha_3^2 - \alpha_4}}{\alpha_3 + \alpha_4}, \quad \Lambda_{\pm} = -m_g^2(1 - X_{\pm})[3 - X_{\pm} + \alpha_3(1 - X_{\pm})]. \quad (21)$$

(See Ref. [33] or Appendix B for derivation.) Note that the background physical metric follows the Friedmann equation with an effective cosmological constant Λ_{\pm} and thus the universe exhibits self-acceleration if $\Lambda_{\pm} > 0$.

Thanks to the exponential map used to define π^a in (18), the action for cosmological perturbations around the self-accelerating FRW background manifestly respects the background symmetry. This allows us to decompose the perturbations into scalar, vector and tensor parts, according to transformation properties under spatial diffeomorphism. A priori, because of the inclusion of four Stückelberg fields, we might expect cosmological perturbations in the gravity sector to consist of 6 degrees of freedom: 2 tensor, 2 vector and 2 scalar modes. Actually, since the theory is constructed in such a way that the would-be BD ghost is completely excised, one would instead expect that cosmological perturbations in the gravity sector should consist of 5 degrees of freedom: 2 tensor, 2 vector and 1 scalar modes. Surprisingly enough, the gauge-invariant analysis of the quadratic action in [33] has shown that the scalar and vector degrees have vanishing kinetic terms. Assuming these degrees are non-dynamical, we may integrate them out, then find that in the scalar and vector sectors, gauge-invariant variables constructed from metric and matter perturbations have exactly the same quadratic action as in general relativity.

Hence, for linear perturbations around the self-accelerating FRW background, difference from general relativity arises only in the tensor sector. Assuming that there is no tensor-type contribution from matter fields σ_I for simplicity, the quadratic action for the tensor sector is given by (5) with

$$c_g = 1, \quad M_{GW}^2 = \pm(r - 1)m_g^2 X_{\pm} \sqrt{1 + \alpha_3 + \alpha_3^2 - \alpha_4}, \quad r = \frac{H}{X_{\pm} H_f}. \quad (22)$$

Here, $H \equiv \dot{a}/(Na)$ and $H_f \equiv \dot{\alpha}/(n\alpha)$ are Hubble expansion rates of the background physical metric and the fiducial metric, respectively. Note that r and thus M_{GW} are time-dependent functions determined by the ratio H/H_f .

We have derived the model described in the previous section with $c_g = 1$. As already stated, the derivation is purely classical and fails at the quantum level [31]. For this reason we do not consider this construction as a realistic one. Nonetheless, at the very least this shows that the structure of the model is not forbidden by symmetry. It may be worthwhile focusing on new models such as Ref. [35] and/or investigating cosmological perturbations around new classes of cosmological backgrounds such as those found in Ref. [19, 26, 36], towards a successful nonlinear completion.

IV. STOCHASTIC GRAVITATIONAL WAVE SPECTRUM

To clarify the influence of M_{GW} on the observable quantities, we seek approximate solutions to Eq. (9) for a generic $M_{GW}(t)$, by considering super-horizon modes to be frozen and sub-horizon modes to follow the WKB-type evolution. We then derive approximate analytic formulas for the energy and power spectra. For simplicity we set

$$c_g = 1, \quad (23)$$

throughout this and the forthcoming sections except for Sec. IV E 4, where we give a brief comment on the case of a general c_g .

A. Horizon re-entry

From the action (5) and the equation of motion (9) with $c_g = 1$, one can easily read off the dispersion relation as

$$\omega^2 = \frac{k^2}{a^2} + M_{GW}^2, \quad (24)$$

where ω is the effective frequency with respect to the proper time τ defined by $d\tau = Ndt = ad\eta$. Here, since the comoving momentum k appears only through the combination $\sqrt{k^2 + 2K}$, we have renamed this combination as k so that K does not appear explicitly. We shall still call k (after this redefinition) comoving momentum. We assume that the mass squared M_{GW}^2 dominates the right hand side of (24) at late time and that it does not lead to instability, i.e.

$$\partial_t(a^2 M_{GW}^2) > 0, \quad M_{GW}^2 > 0. \quad (25)$$

(See Sec. V and Appendix B for a simple example in which these conditions actually hold.)

The frequency ω given by the dispersion relation (24) is relevant and the tensor mode oscillates with this frequency if and only if it is sufficiently high compared with the cosmic expansion, i.e. $\omega^2 \gg H^2$. On the other hand, when $\omega^2 \ll H^2$, the equation of motion (9) allows a growing solution $\tilde{\gamma}_k \propto a$ and thus $\gamma_k \simeq \text{const.}$ At a given moment of time, a mode with $\omega^2 \gg H^2$ is called *sub-horizon* and a mode with $\omega^2 \ll H^2$ is called *super-horizon*, as usual. For a given mode with comoving momentum k , the time when $\omega^2 \simeq H^2$ is called *horizon crossing*, again, as usual.

We suppose that scale-invariant super-horizon gravitational waves are generated in the early universe, e.g. through inflation. In the present paper we concentrate on the subsequent evolution of gravitational waves, assuming for simplicity that the matter energy density and pressure in the background equation of motion (20) satisfy the strong energy condition ($\rho + 3P > 0$). With this assumption, $a^2\rho$ decreases as the universe expands. Since the curvature term ($3K/a^2$) is small (less than a few percent of $3H^2$) at present time, this implies that the curvature term is negligible throughout the evolution. Hence, before the effective cosmological constant Λ_{\pm} starts dominating the universe,² a^2H^2 decreases as the universe expands and, under the assumption (25), super-horizon modes generated in the early universe eventually cross the horizon and become sub-horizon. This type of horizon crossing is called *horizon re-entry*, as usual.

For a mode with comoving momentum k , the time of horizon re-entry is denoted as $t = t_k$ and defined as the solution to

$$\omega^2(t_k) = H^2(t_k). \quad (26)$$

We denote the values of a and H at $t = t_k$ as a_k and H_k , respectively. For comparison, we define the time of horizon re-entry in the massless case (GR) t_k^{GR} by

$$\frac{k^2}{a^2} = H^2 \quad \text{at} \quad t = t_k^{GR}, \quad (27)$$

and denote the values of a and H at $t = t_k^{GR}$ as a_k^{GR} and H_k^{GR} , respectively.

B. Classification of modes

As defined above, the modes re-enter the horizon when the effective frequency ω given by (24) exceeds the Hubble expansion rate H . Thus, the discussion of the evolution of the modes can be reduced to the determination of the time when either the mass contribution $a M_{GW}$ or the comoving momentum k exceeds the comoving horizon scale aH . Hence, in this subsection, we discuss the evolution of $a M_{GW}$ and aH relative to k .

We define two special scales which characterize classification of the different modes. First, we introduce the critical momentum k_c for which, the horizon crossing occurs at time $t = t_c$, when both the momentum and the mass term contribute equally to the frequency,

$$k_c = a_c M_{GW}(t_c) = a_c H_c / \sqrt{2}, \quad (28)$$

where $a_c \equiv a(t_c)$ and $H_c \equiv H(t_c)$. After the time t_c , the sub-horizon evolution of a mode with $k < k_c$ is completely determined by the mass term. The second scale we define is

$$k_0 \equiv a_0 M_{GW}(t_0), \quad (29)$$

that characterizes the momentum of the mode for which, the mass term starts to dominate from today on, $t > t_0$. If $k_c < k_0$ (or equivalently, by Eq. (25), $t_c < t_0$), then the modes which are affected by the mass term will be within the observable universe today. In Fig. 1, we show the characteristic momenta k_c and k_0 in relation to the evolution.

Throughout this paper we assume that

$$k_c < k_0, \quad a_c < a_0. \quad (30)$$

If $a_c < a_0$ is not satisfied, the effective mass would always be smaller than the Hubble expansion rate all the way down to the present time, and would never affect cosmological evolution of gravitational waves. We also assumed $k_c < k_0$ for simplicity.

With these considerations, we classify the modes depending on their momenta:

² We suppose that the Λ_{\pm} domination starts at around $z = O(1)$ and that the evolution after that does not change gravitational wave spectra significantly.

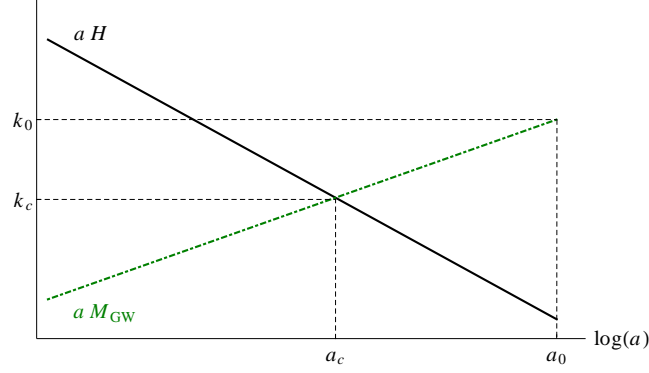


FIG. 1: Schematic plot for the evolution of $a M_{GW}$ and $a H$. We show the critical momentum k_c , defined in (28), for which, the mass and momentum contributions are equal at the time of re-entry, while k_0 , defined in (29), is the momentum of the mode for which the mass term became important just today.

- Short wavelength ($k_0 < k$): modes for which the momentum is large enough to dominate the frequency after horizon re-entry. We thus have $t_k \simeq t_k^{GR}$, $a_k \simeq a_k^{GR}$ and $H_k \simeq H_k^{GR}$. Since the mass term never becomes important, the evolution is indistinguishable from its counterpart in GR.
- Intermediate wavelength ($k_c < k < k_0$): modes for which the mass term becomes dominant after horizon re-entry, but before today. We still have $t_k \simeq t_k^{GR}$, $a_k \simeq a_k^{GR}$ and $H_k \simeq H_k^{GR}$. We expect slight modifications with respect to GR signal.
- Long wavelength ($k < k_c$): modes for which the mass term is dominant at horizon re-entry. Since the momentum is negligible throughout the evolution after horizon exit, their evolution is the same, regardless of their momenta. In other words, t_k for these modes is roughly independent of the momentum and all modes of this type re-enter the horizon simultaneously. We thus have $t_k \simeq t_c$, $a_k \simeq a_c$ and $H_k \simeq H_c$. The largest deviation from general relativity is expected in this category.

This classification is summarized in Fig. 2.

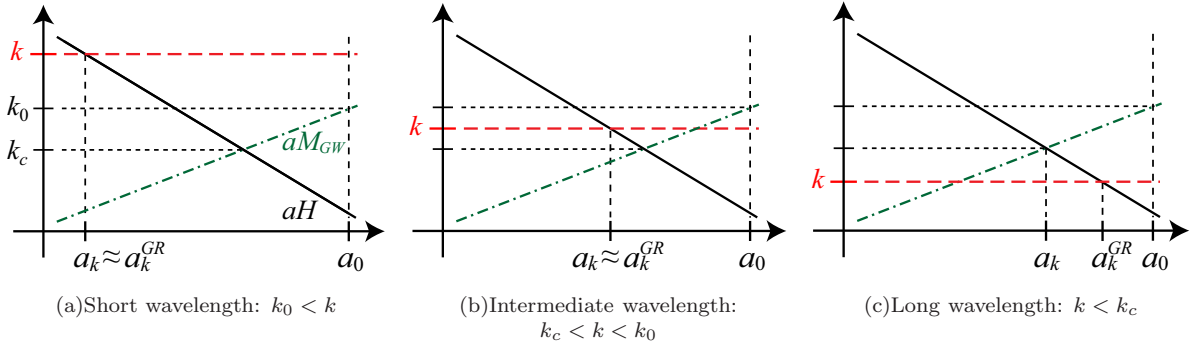


FIG. 2: Examples for each type of momenta based on the classification in the main text. For modes with short and intermediate wavelengths ($k_0 < k$ and $k_c < k < k_0$), the horizon entry time is the same as in GR, with $a_k \sim a_k^{GR}$. However, for modes with long wavelength ($k < k_c$), the momentum term never becomes dominant and the horizon entry in the massive theory occurs earlier than in GR, i.e. $a_k < a_k^{GR}$.

In the forthcoming calculations, especially in subsection IVE, we will need an explicit expression for a_k^{GR} . In order to determine this expression, we use the Friedmann equation for a composite fluid with nonrelativistic matter and radiation, that is,

$$H = \frac{H_{eq}}{\sqrt{2}} \left(\frac{a_{eq}}{a} \right)^2 \sqrt{1 + \frac{a}{a_{eq}}}, \quad (31)$$

where the subscript “eq” denotes the time of matter–radiation equality. (See footnote 2.) Then, the horizon crossing time in GR can be found by solving

$$k^2 = \frac{H_{eq}^2 a_{eq}^4}{2 (a_k^{GR})^2} \left(1 + \frac{a_k^{GR}}{a_{eq}} \right). \quad (32)$$

Depending on the dominant fluid at $t = t_k^{GR}$, the scale factor a_k^{GR} will have a different momentum dependence,

$$\frac{a_k^{GR}}{a_{eq}} = \begin{cases} \frac{k_{eq}^{GR}}{\sqrt{2}k} & \text{for } k \gg k_{eq} \\ \left(\frac{k_{eq}^{GR}}{\sqrt{2}k} \right)^2 & \text{for } k \ll k_{eq} \end{cases}, \quad (33)$$

where $k_{eq}^{GR} \equiv a_{eq} H_{eq}$ is the comoving momentum of the mode which crosses the horizon at the time of equality, in GR.

C. WKB solution

As already stated in subsection IV A, a super-horizon mode stays constant and, thus, its absolute value is given by

$$|\gamma_k| = A(k), \quad \text{for } t < t_k, \quad (34)$$

where $A(k)$ is the amplitude of the mode at the time of its generation, and for slow-roll inflation, is given by

$$A(k) = \frac{H_*}{M_{Pl} k^{3/2}}. \quad (35)$$

Here, H_* is the value of the Hubble expansion rate at the time of horizon exit during inflation.

Once the mode re-enters the horizon at time $t = t_k$, it starts to oscillate with frequency ω . Assuming that the evolution of the frequency is adiabatic, i.e. $\omega^2 \gg H^2$, we can use the WKB approximation to obtain the solution

$$\gamma_k(t) = \frac{C(k)}{\sqrt{\omega(t) a^3(t)}} \exp \left(-i \int \omega a d\eta \right), \quad \text{for } t > t_k, \quad (36)$$

where $C(k)$ is a k -dependent integration constant. By using the thin-horizon approximation, with which we suppose the mode re-enters the horizon sufficiently fast, we can match the super-horizon frozen solution (34) and the sub-horizon oscillating solution (36) at $t = t_k$, resulting in

$$\frac{|\gamma_k(t)|}{A(k)} = \sqrt{\frac{\omega_k}{\omega(t)} \frac{a_k^3}{a^3(t)}}, \quad \text{for } t > t_k, \quad (37)$$

where $\omega_k \equiv \omega(t_k) = H_k$.

For comparison, the corresponding solution in the massless case (GR) is obtained by simply replacing $\omega \rightarrow k/a$ and $t_k \rightarrow t_k^{GR}$ as

$$\frac{|\gamma_k^{GR}(t)|}{A(k)} = \frac{a_k^{GR}}{a(t)}, \quad \text{for } t > t_k^{GR}. \quad (38)$$

D. Power spectrum

Observationally speaking, what we are interested in is the amplitude of sub-horizon gravitational waves today as a function of frequency. We thus would like to compare the amplitude of sub-horizon gravitational waves in massive gravity with that in GR at the same frequency today. For this purpose we define the power spectrum of sub-horizon gravitational waves as

$$\mathcal{P}(\omega_0) \equiv \frac{d}{d \ln \omega_0} \langle \gamma_{ij} \gamma^{ij} \rangle \Big|_{t=t_0} = \frac{\omega_0^2}{\omega_0^2 - M_{GW,0}^2} \frac{2k^3}{\pi^2} |\gamma_k(t_0)|^2, \quad k = a_0 \sqrt{\omega_0^2 - M_{GW,0}^2}, \quad (39)$$

where

$$\omega_0 = \omega(t_0), \quad M_{GW,0} = M_{GW}(t_0), \quad (40)$$

and we have used

$$\frac{d \ln k}{d \ln \omega_0} = \frac{\omega_0^2}{\omega_0^2 - M_{GW,0}^2}. \quad (41)$$

The power spectrum in GR with the same frequency is

$$\mathcal{P}_{GR}(\omega_0) = \frac{2k'^3}{\pi^2} |\gamma_{k'}^{GR}(t_0)|^2, \quad k' = a_0 \omega_0, \quad (42)$$

where k' corresponds to the momentum of the mode in GR with frequency ω_0 .

By using the WKB solution given in the previous subsection, we obtain

$$\mathcal{P}(\omega_0) = \left(\frac{k' a_k}{k a_0} \right)^2 \frac{\omega_k a_k}{\omega_0 a_0} \mathcal{P}_{prim}(k), \quad (43)$$

and

$$\mathcal{P}_{GR}(\omega_0) = \left(\frac{a_{k'}^{GR}}{a_0} \right)^2 \mathcal{P}_{prim}(k'), \quad (44)$$

where we have defined the primordial power spectrum by

$$\mathcal{P}_{prim}(k) \equiv \frac{2k^3}{\pi^2} A^2(k). \quad (45)$$

E. Enhancement of gravitational waves and cutoff

We are interested in the ratio of the power spectrum in massive gravity to that in GR at the same frequency today ω_0 . From the results in the previous subsection, we obtain

$$\frac{\mathcal{P}(\omega_0)}{\mathcal{P}_{GR}(\omega_0)} = \frac{\mathcal{P}_{prim}(k)}{\mathcal{P}_{prim}(k')} \mathcal{S}^2(\omega_0), \quad (46)$$

where

$$\mathcal{S}(\omega_0) = \frac{k' a_k}{k a_{k'}^{GR}} \sqrt{\frac{\omega_k a_k}{\omega_0 a_0}}, \quad k = a_0 \sqrt{\omega_0^2 - M_{GW,0}^2}, \quad k' = a_0 \omega_0. \quad (47)$$

In the rest of this subsection, we estimate the enhancement factor $\mathcal{S}(\omega_0)$ for the three classes of modes introduced in subsection IV B.

1. Short wavelength modes: $k_0 \ll k$

For these small-scale gravitational waves, the frequency ω defined by (24) is dominated by the momentum throughout the evolution, i.e. $\omega \simeq k/a$. Thus we have

$$\omega_k \simeq \frac{k}{a_k}, \quad \omega_0 \simeq \frac{k}{a_0}, \quad k' \simeq k. \quad (48)$$

Also, as illustrated in Fig. 2(a), the horizon re-entry occurs at the same time as in the GR analogue,

$$a_k \simeq a_k^{GR} \simeq a_{k'}^{GR}. \quad (49)$$

Thus, this case does not give rise to an enhancement:

$$\mathcal{S}(\omega_0) \simeq 1. \quad (50)$$

2. *Intermediate wavelength modes: $k_c \ll k \ll k_0$*

For the intermediate-scale gravitational waves, frequency at the time of horizon re-entry is dominated by momentum,

$$\omega_k \simeq \frac{k}{a_k}, \quad (51)$$

giving rise to the same re-entry time as in GR

$$a_k \simeq a_k^{GR}. \quad (52)$$

On the other hand, the mass term comes to dominate at later time, yielding for the frequency of the modes today

$$\omega_0 \simeq M_{GW,0} = \frac{k_0}{a_0}, \quad k' \simeq k_0. \quad (53)$$

Thus, these modes will undergo an enhancement:

$$\mathcal{S}(\omega_0) \simeq \frac{a_k^{GR}}{a_{k_0}^{GR}} \sqrt{\frac{k_0}{k}}. \quad (54)$$

By using the formula (33), we obtain

$$\mathcal{S}(\omega_0) \simeq \begin{cases} \sqrt{\frac{k_0^3}{k^3}} \simeq \left(\frac{\omega_0^2}{M_{GW,0}^2} - 1 \right)^{-3/4} & \text{for } k_{eq} \ll k \ll k_0 \\ \sqrt{\frac{k_{eq}^2 k_0^3}{2k^5}} \simeq \frac{k_{eq}}{\sqrt{2}k_0} \left(\frac{\omega_0^2}{M_{GW,0}^2} - 1 \right)^{-5/4} & \text{for } k \ll k_{eq} \ll k_0 \\ \sqrt{\frac{k_0^5}{k^5}} \simeq \left(\frac{\omega_0^2}{M_{GW,0}^2} - 1 \right)^{-5/4} & \text{for } k \ll k_0 \ll k_{eq} \end{cases}. \quad (55)$$

3. *Long wavelength modes: $k \ll k_c$*

When these modes re-enter the horizon, the mass term is already dominant in their frequency

$$\omega_k \simeq M_{GW}(t_k), \quad (56)$$

and thus the re-entry time is independent of the comoving momentum. In other words, all modes with $k \ll k_c$ re-enter the horizon simultaneously when the Hubble expansion rate and the effective mass of gravitational waves agree

$$H(t_k) \simeq M_{GW}(t_k). \quad (57)$$

Up to factors of order one, this is essentially the definition of t_c introduced in subsection IV B and thus $t_k \simeq t_c$. Hence, we have

$$a_k \simeq a_c, \quad \omega_c \simeq M_{GW}(t_c) = \frac{k_c}{a_c}. \quad (58)$$

Since we have assumed that aM_{GW} is a growing function of time, M_{GW} dominates ω at $t = t_0$ as well:

$$\omega_0 \simeq M_{GW,0} = \frac{k_0}{a_0}, \quad k' \simeq k_0. \quad (59)$$

Thus we obtain

$$\mathcal{S}(\omega_0) \simeq \frac{a_c}{a_{k_0}^{GR}} \frac{\sqrt{k_0 k_c}}{k} \simeq \frac{a_c}{a_{k_0}^{GR}} \sqrt{\frac{k_c}{k_0}} \left(\frac{\omega_0^2}{M_{GW,0}^2} - 1 \right)^{-1/2}. \quad (60)$$

4. Summary of enhancement factor

As one can see from the schematic plot in Fig. 3, qualitative behavior of the amplification factor $\mathcal{S}(\omega_0)$ is summarized as follows.

- No modification in the high frequency range ($k_0 < k \Leftrightarrow \sqrt{2}M_{GW,0} < \omega_0$): $\mathcal{S}(\omega_0)$ stays almost unity.
- Modest enhancement in the intermediate frequency range ($k_c < k < k_0 \Leftrightarrow \omega_c < \omega_0 < \sqrt{2}M_{GW,0}$): $\mathcal{S}(\omega_0)$ is proportional to some positive powers of $(\omega_0^2 - M_{GW,0}^2)^{-1}$, and thus increases as ω_0 decreases.
- Sharp peak just above the cutoff ($0 < k < k_c \Leftrightarrow M_{GW,0} < \omega_0 < \omega_c$): $\mathcal{S}(\omega_0)$ is proportional to $(\omega_0^2 - M_{GW,0}^2)^{-1/2}$, and thus it diverges in the limit $\omega_0 \rightarrow M_{GW,0}$.
- No signal below the cutoff ($\omega_0 < M_{GW,0}$): $\mathcal{S}(\omega_0) = 0$.

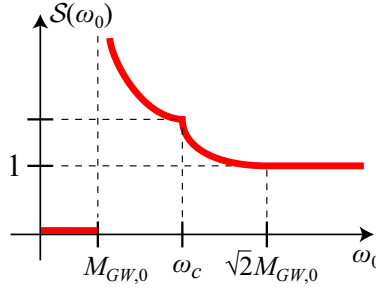


FIG. 3: Schematic plot of the amplification factor $\mathcal{S}(\omega_0)$.

We emphasize that the qualitative feature of the spectrum shown in Fig. 3 is quite universal; as long as $a M_{GW}$ is an increasing function of time and the two scales $k_c < k_0$ are well separated, it applies to any fiducial metric, or even other models of massive gravity.

Before going into the next subsection, we briefly comment on the case where c_g is not constant.³ We assume that $c_g k/a$ becomes equal to each of H and M_{GW} only once, similarly to the case of constant c_g we have discussed. In this case, Eqs. (24) are altered into (28) and (29) into

$$\omega^2 = \frac{c_g(t)k^2}{a^2} + M_{GW}^2, \quad c_g(t_c)k_c = a_c M_{GW}(t_c) = a_c H_c, \quad c_g(t_0)k_0 = a_0 M_{GW}(t_0). \quad (61)$$

We redefine the horizon crossing time t_k using ω in this equation. Using these new definitions, we may repeat the derivations in the previous subsections to obtain the formula for $\mathcal{S}(\omega_0)$. Its expression is given by

$$\mathcal{S}(\omega_0) = \frac{k' a_k}{c_g(t_0)k a_{k'}^{GR}} \sqrt{\frac{\omega_k a_k}{\omega_0 a_0}} \simeq \begin{cases} \frac{a_k}{a_{c_g(t_0)k}^{GR}} \sqrt{\frac{c_g(t_k)}{c_g(t_0)}} & (k_0 \ll k) \\ \frac{a_k}{a_{c_g(t_0)k_0}^{GR}} \sqrt{\frac{c_g(t_k)k_0}{c_g(t_0)k}} & (k_c \ll k \ll k_0) \\ \frac{a_c}{a_{c_g(t_0)k}^{GR}} \sqrt{\frac{c_g(t_c)k_0 k_c}{c_g(t_0)k^2}} & (k \ll k_c) \end{cases} \quad (62)$$

Note that also the primordial spectrum $\mathcal{P}_{prim}(k)$ may be shifted if $c_g(t)$ is shifted from the unity in the inflationary era.

³ Note that c_g is bounded from below as $c_g - 1 \gtrsim -10^{-15}$ if we take into account the gravitational Cherenkov radiation [37, 38]. See also, e.g., Refs. [39, 40] for models which may give $c_g \neq 1$.

F. Signatures in the spectrum

In the previous subsection, we have shown that the enhancement factor $\mathcal{S}(\omega_0)$ defined by (46) diverges in the limit $\omega_0 \rightarrow M_{GW,0} + 0$. However, the power spectrum $\mathcal{P}(\omega_0)$ itself does not diverge, provided that

$$\lim_{k \rightarrow +0} k^{-2} \mathcal{P}_{prim}(k) < \infty. \quad (63)$$

This is the case, for example, if the primordial gravitational waves are generated by inflation in the early universe and if the e-folding number of the inflation is finite. Nonetheless, from the divergence of $\mathcal{S}(\omega_0)$ it is likely that the power spectrum $\mathcal{P}(\omega_0)$ has a sharp peak just above the cutoff at $\omega_0 = M_{GW,0}$. Below the cutoff, the power spectrum should vanish.

The peak just above $\omega_0 = M_{GW,0}$ may become rather high if the primordial spectrum $\mathcal{P}_{prim}(k)$ of gravitational waves continues to a far infrared. For example, this situation can be realized when the duration of inflation is prolonged. Concretely, $\mathcal{P}_{prim}(k)$ is expected to continue down to $k \sim a_0 H_0 e^{-N_{extra}}$, where N_{extra} is the number of additional e-folds to the minimum needed for the spatial curvature to stay below the observational bounds. Hence, by the formula (60), the enhancement factor at the peak is estimated as

$$\mathcal{S}_{peak} \sim \frac{a_c}{a_{k_0}^{GR}} \frac{\sqrt{k_0 k_c}}{a_0 H_0} e^{N_{extra}}. \quad (64)$$

Future observation of gravitational waves may reveal deviation from the spectrum predicted by GR. If the cutoff and the sharp peak just above it are found, then this might be a signature of massive gravity. In this case, from the frequency at the cutoff one can read off the value of $M_{GW,0}$. It might also be possible to read off some information about the fall-off behavior of the primordial spectrum in the far infrared (63), from the height of the peak.

V. NUMERICAL RESULTS

In the previous section we have shown that the power spectrum of stochastic gravitational waves in massive gravity vanishes at frequencies below a cutoff and a sharp peak is expected just above the cutoff. The cutoff frequency agrees with the effective mass of gravitational waves today $M_{GW,0}$. It is therefore interesting if the effective mass $M_{GW,0}$ is within the frequency range to which gravitational wave detectors are sensitive. For example, space-based gravitational observatories like the Laser Interferometer Space Antenna (LISA) [41] is sensitive to the frequency range $10^{-4} - 1$ Hz. The DECi-hertz Interferometer Gravitational wave Observatory (DECIGO) [42] has better sensitivity in the frequency range $10^{-1} - 1$ Hz. For lower frequencies, pulsar timing arrays such as the Square Kilometre Array (SKA) [43] and the Parkes Pulsar Timing Array (PPTA) [44] have sensitivities down to 10^{-8} Hz. The combined sensitivity range for these observatories is thus $10^{-8} - 1$ Hz. Thus, using these observatories, one might be able to hope future detection of the cutoff and the peak in the gravitational wave spectrum if

$$10^{-8} \text{ Hz} < M_{GW,0} < 1 \text{ Hz}. \quad (65)$$

The spectrum obtained analytically in the previous section, especially its peak structure, is not sensitive to the history of $M_{GW}(t)$ in the early universe but is essentially determined by its present value $M_{GW,0}$. Thus, for the purpose of numerical calculations, we consider time-independent $M_{GW} = M_{GW,0}$ in the range (65).⁴

In Fig. 4, we compare the numerically obtained gravitational wave spectrum and the analytic estimation derived in the previous section. The former is obtained by numerically solving Eq. (9) with the mass term assumed to be $M_{GW,0} = 10^{10} H_0 \sim 2 \times 10^{-7}$ Hz, for which we find $k_0/H_0 = 10^{10}$ and $k_c/H_0 \sim 10^4$. The evolution of the gravitational wave inside the Hubble or mass horizon is calculated using the WKB solution, Eq. (36), in order to save computational time. The latter is obtained by multiplying the numerically obtained spectrum in GR by the analytically obtained factor $\mathcal{S}(\omega_0)$, given in Eq. (62). In both cases, we assume that the evolution of the Hubble expansion rate is determined by the density parameters of radiation $\Omega_r h^2 = 4.15 \times 10^{-5}$, matter $\Omega_m h^2 = 0.1344$, and cosmological constant (either the genuine cosmological constant or the effective one induced by the graviton mass term, or their sum) $\Omega_\Lambda = 0.734$,

⁴ Note that in Sec. II we have assumed that propagating degrees of freedom in the gravity sector are the two tensor modes only. This means that the scalar and vector parts of linear perturbations behave exactly like GR and thus there is no constraint from modification of Newtonian potential as far as linear perturbation is a good approximation. See e.g. Refs. [45, 46] for the discussions and bound on the graviton mass when those degrees of freedom are taken into account.

with the normalized Hubble rate $h = 0.71$ [47]. The primordial spectrum is assumed to be scale-invariant and its amplitude is normalized by $\mathcal{P}_{\text{prim}}(k) = 2.43 \times 10^{-10}$, where we assumed the tensor-to-scalar ratio to be 0.1 and the amplitude of the scalar primordial spectrum to be 2.43×10^{-9} [47]. We also suppose that the primordial spectrum have an IR cutoff at $k/(a_0 H_0) = e^{-N_{\text{extra}}} = 10^{-1}$. We can clearly see that the numerical result matches almost exactly the analytic result derived in Sec. IV, and the peak height is well described by Eq. (64), which gives $\mathcal{S}_{\text{peak}} \sim 10^{15}$.

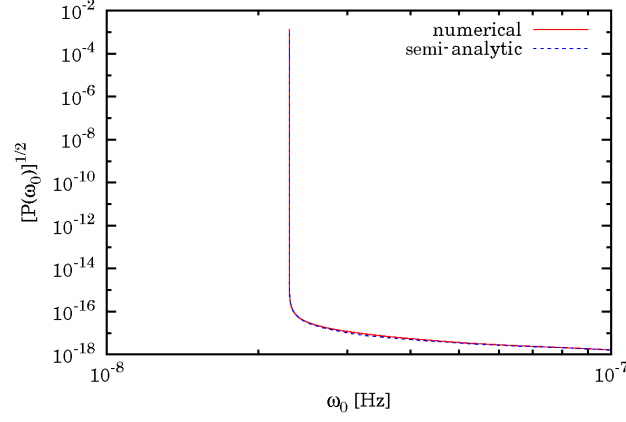


FIG. 4: Gravitational power spectrum in the massive gravity with $M_{GW,0} = 10^{10} H_0 \sim 2 \times 10^{-7}$ Hz shown with respect to ω_0 . The solid (red) curve is the spectrum obtained by the numerical calculation, and the dashed (blue) curve is the semi-analytical spectrum given by Eq. (46), where the GR spectrum is calculated numerically and the enhancement factor $\mathcal{S}(\omega_0)$ is given analytically by Eqs. (50), (55) and (60).

Since the plot in Fig. 4 is shown with respect to $\omega_0 \sim [(k/a_0)^2 + M_{GW,0}^2]^{1/2}$, most of the peak structure in the spectrum is compressed to a narrow region at $\omega_0 \sim M_{GW,0}$ and its detailed structure is too subtle to see. To make the fine structure of the peak manifest, we show the plots with respect to k in Fig. 5. We can see that the k dependence changes at k_0 and k_c as prescribed in Sec. IV, and that the semi-analytical result well reproduces the numerical one.

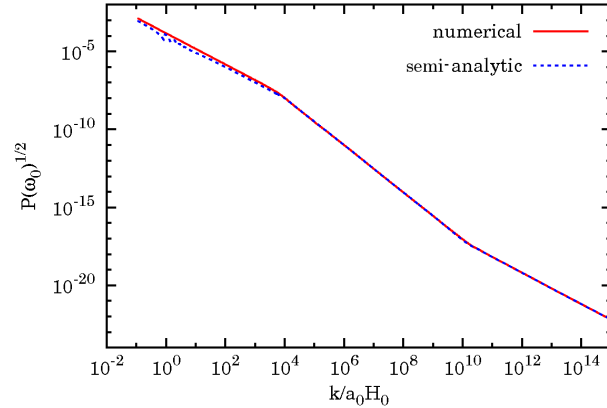


FIG. 5: The gravitational power spectra in the massive gravity theory with $M_{GW,0} = 10^{10} H_0 \sim 2 \times 10^{-7}$ Hz shown with respect to $k/a_0 H_0$. The spectra are obtained by the numerical calculation (solid red) and semi-analytic estimate by Eqs. (46), (50), (55) and (60) (dotted blue), respectively. For the latter, the GR spectrum is calculated numerically and the enhancement factor $\mathcal{S}(\omega_0)$ is calculated analytically.

Before closing this section, we briefly comment on the observability of the peak feature in the spectrum. As seen from Fig. 6, the peak is observable by the pulsar timing or eLISA, and/or DECIGO if the mass is in the range of Eq. (65). For example, for the case of $M_{GW,0} = 10^{-8}$ Hz and a primordial spectrum with an IR cutoff at $k/a_0 = 1/H_0$, we find that the enhancement factor $\mathcal{S}(\omega_0)$ reaches $\sim 10^{13}$. Since the enhancement is so large, we can expect the peak to be observable even when the tensor-to-scalar ratio takes much smaller value. If $M_{GW,0}$ is much larger than 1 Hz, the peak in the spectrum would be more manifest, and the signal would be observable even for ground-based

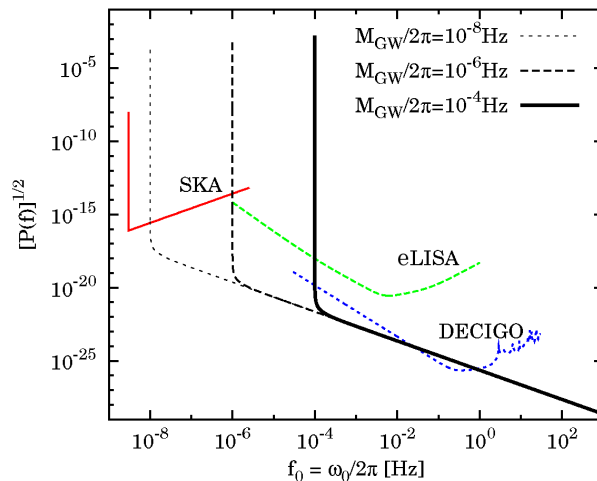


FIG. 6: Gravitational power spectra for $M_{GW,0}/2\pi = 10^{-8}, 10^{-6}, 10^{-4}$ Hz shown with sensitivity curves of future experiments. The curves are plotted assuming 10-year runs of pulsar timing array with SKA [48], the single detector sensitivity of eLISA [49], and the cross-correlation analysis of a 3-year observation with DECIGO [42]. For the primordial spectra, we consider the tensor-to-scalar ratio to be 0.1 and $e^{-N_{extra}} = 10^{-1}$.

observatories, such as LIGO or KAGRA [50, 51].

Note that, due to the finiteness of the observation time T_{obs} , the observed peak in the Fourier space is smoothed with a width of $\Delta f \sim 1/T_{obs}$. The signal would be detectable even after taking this effect into account if the amplification is sufficiently large. For example, following the calculations in Ref. [52] which discussed the pulsar timing observations, we find that the total RMS fluctuation of the timing residuals induced by the stochastic gravitational wave background is amplified relative to GR by a factor $\sim 10^{-4} \times (T_{obs}/H_0)^{-4} (M_{GW,0}/H_0)^{-3} \log(e^{N_{extra}} M_{GW,0}/H_0)$. For $M_{GW,0} \gtrsim 10^{-8}$ Hz, this factor becomes large enough for the signal to be detectable by the cross correlation analysis using PPTA argued in Ref. [52] unless the tensor-to-scalar ratio is extremely small.

VI. SUMMARY AND DISCUSSIONS

In this paper, we discussed how to probe the graviton mass using the gravitational wave observations. Our results are based on a general quadratic action given by Eq. (5) in which the graviton mass can be time-dependent, and thus they apply universally to any massive gravity theories in which modification from GR appears primarily in the tensor modes. The salient feature of the result is the sharp peak in the gravitational wave spectrum, whose position and height may tell us about the graviton mass of today and the length of the inflationary period. In Sec. V, we confirmed our analytical results match well with the numerical results which do not assume the thin-horizon approximation, and also argued the observability of the gravitational wave signal for various observatories. It would be interesting to apply the results to explicit examples of nonlinear completion of massive gravity theories and to derive constraints on such models based on the gravitational wave observations.

Although the example discussed in Sec. III (as well as in Ref. [33]) was recently shown to suffer from nonlinear instabilities [31], it is expected that other working examples exist. A construction with no extra polarization with respect to GR was discussed in [30], where a constant mass contribution appears in the dispersion relations of the gravitational waves. Another potential example is the scenario considered in [35], where the scalar mode is rendered redundant by introduction of some symmetry. Although the vector graviton degrees are still present in this construction, the lack of the scalar graviton would relax the bounds from solar system tests.

Below, we briefly discuss other probes which are sensitive to $M_{GW}(t)$ at the time other than today. One interesting probe is the cosmic microwave background (CMB), especially its B-mode polarization spectrum which is sourced solely by gravitational waves. The signatures in CMB spectrum in the case of the constant mass M_{GW} was discussed by Ref. [53]. Following the argument to derive the B-mode spectrum and generalizing it to the case of time-dependent mass term, we find that the main contribution to the spectrum is sensitive to the value of the mass at the time of the

recombination⁵. The most interesting observational feature will be obtained when the graviton mass at that time is in the range $(10\text{Mpc})^{-1} < M_{GW} < (10\text{Kpc})^{-1}$. For such a value of M_{GW} , the contribution to the B-mode spectrum from the gravitational wave increases compared to the GR case for the modes of low angular multipole ℓ , and a plateau in the spectrum up to $\ell \lesssim 10^{-3} \times M_{GW}/H_0 \sim 100$ is expected to emerge. There will be no signal for smaller values of M_{GW} , while for larger values, the entire spectrum will be suppressed, since the rapid oscillation of the gravitational wave, driven by the large M_{GW} , will average out the contribution to the CMB polarization spectrum.

Another interesting probe of the modification in tensor sector of gravity is the inspiralling compact binaries; the changes in the propagation speed due to the mass term will give rise to a modification in the evolution of the phase of the gravitational waves emitted by those binaries. Such an effect and the constraint on the constant graviton mass are argued in Ref. [54]. It may be interesting to generalize this analysis to the case of time-dependent graviton mass and discuss its observability for the future-planned gravitational wave observatories.

Finally, we give a brief comment on the time evolution of the gravitational wave energy density and a possible constraint on it. The energy spectrum of the gravitational wave defined with respect to wavenumber k is given by

$$\Omega_{GW}(k, t) = \frac{1}{\rho_{\text{crit}}} \frac{d\rho_{GW}}{d\log k} = \frac{k^3}{12\pi H^2} (N^{-2} \dot{\gamma}_k^2 + \omega^2 \gamma_k^2) \propto k^3 \omega^2 \gamma_k^2, \quad (66)$$

where ω is given by Eq. (24) and the final expression is valid for the WKB solution of Eq. (36). The ratio of the energy spectrum of the massive gravity relative to GR can be obtained following the derivations similar to Sec. IV. To discuss the constraint on the gravitational wave energy density coming from the Big Bang nucleosynthesis (BBN), we need to do the analysis taking t to be the time of BBN. We assume that the gravitational wave primordial amplitude is given by Eq. (35), and consider the case that $M_{GW}(t)$ becomes larger than the Hubble scale before BBN. In such a case, the ratio is given by

$$\frac{\Omega_{GW}(k)}{\Omega_{GW}^{GR}(k)} = \begin{cases} 1 & (k_0 < k) \\ k_0/k & (k_c < k < k_0) \\ k_0/k_c & (k < k_c) \end{cases}, \quad (67)$$

where k_0 and k_c are defined in a similar manner with Sec. IV replacing t_0 by t_{BBN} . Roughly speaking, the total energy density of the gravitational wave becomes larger than that in GR by a factor of $k_0/k_c = M_{GW}(t_{\text{BBN}})/\sqrt{H_{\text{BBN}} M_{GW}(t_c)}$ if k_c is sufficiently large. Since the total energy density must satisfy $\int d(\log k) \Omega_{GW}(k) < 10^{-5}$ at least [55], this enhancement of the gravitational wave energy density may give a tighter constraint on the primordial amplitude of the gravitational wave or the inflationary models from which it is derived. Obviously this constraint will be sensitive to $M_{GW}(t_{\text{BBN}})$. It may be interesting to pursue this issue using explicit examples of the massive gravity theories.

Acknowledgments

We thank G. D’Amico, C. de Rham, N. Kaloper, A. Taruya and A. J. Tolley for useful discussions. We are also grateful to the organizers and participants of the YITP workshop YITP-T-12-04 “Nonlinear massive gravity theory and its observational test” for hospitality and useful comments. The work of A.E.G., C.L. and S.M. is supported by the World Premier International Research Center Initiative (WPI Initiative), MEXT, Japan. S.M. also acknowledges the support by Grant-in-Aid for Scientific Research 24540256 and 21111006, and by Japan-Russia Research Cooperative Program. N.T. is supported in part by the DOE Grant DE-FG03-91ER40674. S.K. is supported by the Grant-in-Aid for Scientific Research No. 23340058 and No. 24740149.

Appendix A: Example from nonlinear massive gravity

In the nonlinear theory of massive gravity, the mass term not only introduces the effective mass to gravitational waves but also drives self-accelerating universes. In order to attribute the late-time acceleration of our universe to

⁵ We find the contribution of the gravitational wave to the CMB B-mode spectrum is roughly proportional to $\int^{\eta_r} (k^2 + a^2 M_{GW}(\eta)) d\eta$, where η_r is the conformal time at the time of the recombination. In a generic case, this value is sensitive to $M_{GW}(\eta_r)$ rather than $M_{GW}(\eta)$ at any other η .

the self-acceleration from massive gravity, the effective cosmological constant Λ_{\pm} due to the mass term should be set to the observed value:

$$\Lambda_{\pm} \sim H_0^2. \quad (\text{A1})$$

Therefore, a relevant question now is whether the nonlinear theory of massive gravity can simultaneously accommodate the effective mass in the preferred range (65) and the preferred value of the effective cosmological constant (A1). These two quantities are given by the formulas (22) and (21), respectively. (For the sign of the effective cosmological constant in each branch, see Figure 1 of Ref. [33].) Thus, for generic values of the parameters α_3 and α_4 , the graviton mass m_g in the action should be

$$m_g \sim H_0, \quad (\text{A2})$$

and the quantity $r = H/(X_{\pm}H_f)$ at present must be in the range

$$10^{20} < r_0 < 10^{28}. \quad (\text{A3})$$

where $r_0 \equiv r(t_0)$.

If we suppose that the primordial spectrum $\mathcal{P}_{prim}(k)$ of gravitational waves is generated by inflation then in order for the inflationary mechanism of generation of quantum fluctuations to work, the effective mass of gravitational waves must be sufficiently lower than the Hubble expansion rate during inflation. This is translated to the condition

$$r \ll \frac{H_I^2}{H_0^2} \quad \text{during inflation}, \quad (\text{A4})$$

where H_I is the Hubble expansion rate during inflation.

For example, if we demand the Poincaré symmetry in the field space as a global symmetry of the theory then the fiducial metric is restricted to Minkowski and the FRW background of the physical metric is inevitably an open universe [18]. In this case we have

$$r = \frac{Ha}{\sqrt{|K|}}, \quad (\text{A5})$$

where K (< 0) is the spatial curvature constant. It is evident that r increases during inflation and decreases after that (see footnote 2). Hence, the condition (A3) implies that $r \gg 1$ throughout the evolution after inflation. In this case $M_{GW}^2 \sim r m_g^2$ for the '+' branch (or $M_{GW}^2 \sim -r m_g^2$ for the '-' branch), and the assumption (25) is actually satisfied, provided that $P \leq \rho$ and $m_g^2 > 0$ (or $m_g^2 < 0$, respectively).

Since r decreases after inflation, the condition (A4) leads to an upper bound on r_0 . We thus need to see if such an upper bound on r_0 is consistent with the preferred range (A3). For this purpose, supposing that the universe is dominated by inflaton oscillation (with the effective equation of state parameter $w = 0$) between the end of inflation ($a = a_f$) and the onset of the radiation dominated epoch ($a = a_R$), the scale factor today is estimated by the entropy conservation as

$$\frac{a_0}{a_f} \sim g^{1/12} \frac{\sqrt{M_{Pl}H_I}}{T_0} \left(\frac{a_R}{a_f} \right)^{1/4}, \quad (\text{A6})$$

where T_0 is the photon temperature today and g is the number of relativistic degrees of freedom that eventually inject entropy to photons. By using this formula, the bound (A4) at the end of inflation $t = t_f$ is rewritten as

$$r_0 = r_f \frac{H_0}{H_I} \frac{a_0}{a_f} \ll \frac{H_I}{H_0} \frac{a_0}{a_f} \sim g^{1/12} \frac{\sqrt{M_{Pl}H_I}}{T_0} \frac{H_I}{H_0} \left(\frac{a_R}{a_f} \right)^{1/4}, \quad (\text{A7})$$

where $r_f = r(t_f)$. For example, for $g^{1/12} = O(1)$ with the instantaneous reheating approximation $a_R \simeq a_f$, this leads to

$$r_0 \ll 10^{84} \times \left(\frac{H_I}{10^{13} \text{GeV}} \right)^{3/2}, \quad (\text{A8})$$

and is consistent with the preferred range (A3). Thus, in this simple example with Minkowski fiducial metric, the range (A3) is consistent with the inflationary generation mechanism of primordial gravitational waves.

Note that, by the formula (A5), the extreme hugeness of r_0 implied by the preferred range (A3) is translated to the extreme flatness of our universe today: $10^{-56} < |\Omega_{tot} - 1| < 10^{-40}$. Thus, the number of e-folds during inflation must be much more than what is needed to solve the flatness problem. The preferred range (A3) corresponds to the number of extra e-folds $\sim \ln r_0$ in the range

$$45 < N_{extra} < 65. \quad (\text{A9})$$

With this large number of extra e-folds, the primordial spectrum $\mathcal{P}_{prim}(k)$ of gravitational waves is expected to continue to a far infrared. Therefore, from the discussion in subsection IV F we conclude that the peak just above $\omega_0 = M_{GW,0}$ should be rather high. Concretely, $\mathcal{P}_{prim}(k)$ is expected to continue down to $k \sim a_0 H_0 e^{-N_{extra}}$. By the formula (60), this corresponds to the large enhancement at the peak,

$$\mathcal{S}_{peak} \sim \frac{a_c}{a_{k_0}^{GR}} \frac{\sqrt{k_0 k_c}}{a_0 H_0} e^{N_{extra}} \sim \frac{a_c}{a_{k_0}^{GR}} \frac{\sqrt{k_0 k_c}}{a_0 H_0} r_0. \quad (\text{A10})$$

Appendix B: General fiducial metric

1. FRW-type fiducial metric

The background equation of motion for a general fiducial metric is derived in the Appendix A.1 of Ref. [33]. We briefly summarize that derivation for reference.

We consider a FRW-type fiducial metric given by

$$f_{\mu\nu} = -\hat{n}^2(\hat{\phi}^0) \partial_\mu \hat{\phi}^0 \partial_\nu \hat{\phi}^0 + \hat{\alpha}^2(\hat{\phi}^0) \Omega_{ij}^{(K)} \partial_\mu \hat{\phi}^i \partial_\nu \hat{\phi}^j, \quad (\text{B1})$$

where \hat{n} and $\hat{\alpha}$ are general functions of $\hat{\phi}^0$. Applying the field redefinition given by $(\hat{\phi}^0, \hat{\phi}^i) = (f(\phi^0), \phi^i)$, where f is a function to be determined, and taking the gauge $\phi^\mu = x^\mu$, the fiducial metric of Eq. (B1) becomes

$$f_{\mu\nu} dx^\mu dx^\nu = -\hat{n}^2(f(t)) \dot{f}(t)^2 dt^2 + \hat{\alpha}^2(f(t)) \Omega_{ij}^{(K)} dx^i dx^j, \quad (\text{B2})$$

where the dot ($\dot{}$) denotes the derivative with respect to t . For this fiducial metric, the matrix \mathcal{K}^μ_ν becomes

$$\mathcal{K}^\mu_\nu = \text{Diag}(\zeta, \xi, \xi, \xi), \quad \zeta = 1 - \frac{\hat{n} \dot{f}}{N}, \quad \xi = 1 - \frac{\hat{\alpha}}{a}. \quad (\text{B3})$$

Then, up to boundary terms the gravity action reduces to

$$I_g = \int d^3x \sqrt{\Omega} \left(3KNa - \frac{3a\dot{a}^2}{N} + m_g^2 L_g \right), \quad (\text{B4})$$

where

$$L_g = Na^3 (\mathcal{L}_2 + \alpha_3 \mathcal{L}_3 + \alpha_4 \mathcal{L}_4), \quad \mathcal{L}_2 = 3\xi(\zeta + \xi), \quad \mathcal{L}_3 = \xi^2(3\zeta + \xi), \quad \mathcal{L}_4 = \xi\zeta^3. \quad (\text{B5})$$

The variation of this action with respect to f yields

$$0 = \frac{\partial L_g}{\partial \zeta} \frac{\partial \zeta}{\partial f} + \frac{\partial L_g}{\partial \xi} \frac{\partial \xi}{\partial f} - \left(\frac{\partial L_g}{\partial \zeta} \frac{\partial \zeta}{\partial \dot{f}} \right) = 3Na^2 \left(aH - \alpha \hat{H}_f \right) [1 + 2\xi + \alpha_3(2 + \xi)\xi + \alpha_4\xi^2], \quad (\text{B6})$$

where H and H_f are the Hubble parameters of the physical and fiducial metrics defined by

$$H(t) \equiv \frac{\dot{a}}{Na}, \quad \hat{H}_f(f(t)) \equiv \frac{\hat{\alpha}'}{\hat{n}\hat{\alpha}} \quad \left(\hat{\alpha}' \equiv \frac{d\hat{\alpha}}{d\hat{\phi}^0} \right). \quad (\text{B7})$$

Below, we focus on the solution of Eq. (B6) given by⁶

$$1 + 2\xi + \alpha_3\xi(2 + \xi) + \alpha_4\xi^2 = 0, \quad (\text{B8})$$

⁶ See Refs. [34, 56] for cosmological solutions on the other branch.

whose solution is given by

$$X_{\pm} = 1 - \xi = \frac{\hat{\alpha}(f(t))}{a(t)}, \quad X_{\pm} \equiv \frac{1 + 2\alpha_3 + \alpha_4 \pm \sqrt{1 + \alpha_3 + \alpha_3^2 - \alpha_4}}{\alpha_3 + \alpha_4}. \quad (\text{B9})$$

Varying the action with respect to N and a and using the solution of Eq. (B9), we obtain Eq. (20) as the background equations. The second equation in Eq. (20) is consistent with the first one if the matter fluid obeys usual conservation law $\dot{\rho} + 3(\dot{a}/a)(\rho + p) = 0$. The evolution of a is determined by Eq. (20) for given N , and it determines $f(t)$ via Eq. (B9). Note that $\hat{n}(f(t))$, $\hat{\alpha}(f(t))$ and $\hat{H}_f(f(t))$ correspond to $n(t)$, $\alpha(t)$ and $H_f(t)$ of Sec. II, respectively. (Almost equivalently, we may set $f(t) = t$ and regard $\hat{\alpha}(t)$ and $\hat{n}(t)$ are given functions. In this case, Eq. (B9) and the Friedmann equation in Eq. (20) are regarded as equations to fix $a(t)$ and $N(t)$, respectively.)

One example of the fiducial metric of this type is the Minkowski metric in the open chart ($K < 0$) given by [18]

$$f_{\mu\nu} = -\partial_{\mu}\varphi^0\partial_{\nu}\varphi^0 + \delta_{ij}\partial_{\mu}\varphi^i\partial_{\nu}\varphi^j = -f'^2(\phi^0)\partial_{\mu}\phi^0\partial_{\nu}\phi^0 + |K|f^2(\phi^0)\Omega_{ij}^{(K)}dx^idx^j, \quad (\text{B10})$$

where we used the field redefinition given by

$$\varphi^0 = f(\phi^0)\sqrt{1 - K\delta_{ij}\phi^i\phi^j}, \quad \varphi^i = \sqrt{-K}f(\phi^0)\phi^i. \quad (\text{B11})$$

Taking the gauge $\phi^i = x^i$, we find Eq. (B9) becomes $X_{\pm} = \sqrt{|K|}f(t)/a(t)$, which determines $f(t)$ in terms of $a(t)$. The Friedmann equation, Eq. (20), holds as it is. In this case we have $n(\phi^0) = |f'(\phi^0)|$ and $\alpha(\phi^0) = \sqrt{|K|}f(\phi^0)$, and thus $H_f = \text{sign}(f')/f = \text{sign}(f')\sqrt{|K|}/X_{\pm}a$.

2. (Anti)-de Sitter fiducial metric

In this section, we comment that the fiducial metric of Eq. (17) for any K can be obtained from a single de Sitter metric, and the for $K > 0$ can be obtained from the anti-de Sitter metric.

We begin with the de Sitter fiducial metric with flat spatial section given by

$$f_{\mu\nu} = -\partial_{\mu}\varphi^0\partial_{\nu}\varphi^0 + \exp(2\bar{H}_f\varphi^0)\delta_{ij}\partial_{\mu}\varphi^i\partial_{\nu}\varphi^j. \quad (\text{B12})$$

By the redefinition $\varphi^0 = f(\phi^0)$ and $\varphi^i = \phi^i$, this fiducial metric takes the form of Eq. (17) with $K = 0$, $H_f = \bar{H}_f$, $n = |f'|$ and $\alpha = \exp(2\bar{H}_f f(\phi^0))$.

Assuming $K > 0$, the field redefinition given by

$$\varphi^0 = \bar{H}_f^{-1} \log \left[\sinh f(\phi^0) + \cosh f(\phi^0) \sqrt{1 - K\delta_{ij}\phi^i\phi^j} \right], \quad \varphi^i = \frac{\bar{H}_f^{-1} \sqrt{K}\phi_i}{\tanh f(\phi^0) + \sqrt{1 - K\delta_{ij}\phi^i\phi^j}} \quad (\text{B13})$$

makes the fiducial metric of Eq. (B12) into

$$f_{\mu\nu} = \bar{H}_f^{-2} \left(-f'^2(\phi^0)\partial_{\mu}\phi^0\partial_{\nu}\phi^0 + K \cosh^2 f(\phi^0) \Omega_{ij}^{(K)} \partial_{\mu}\phi^i\partial_{\nu}\phi^j \right), \quad (\text{B14})$$

which is of the form of Eq. (17) with $K > 0$ and $H_f = \bar{H}_f \tanh f(\phi^0)$. The counterpart of Eq. (B9) for Eq. (B14) is given by

$$X_{\pm} = \frac{\sqrt{K} \cosh(f(t))}{\bar{H}_f a(t)}, \quad (\text{B15})$$

and the Friedmann equation, Eq. (20), holds as it is.

Similarly, for $K < 0$, the redefinition given by

$$\varphi^0 = \bar{H}_f \log \left[\cosh f(\phi^0) + \sinh f(\phi^0) \sqrt{1 - K\delta_{ij}\phi^i\phi^j} \right], \quad \varphi^i = \frac{\bar{H}_f^{-1} \sqrt{|K|}\phi^i}{\coth f(\phi^0) + \sqrt{1 - K\delta_{ij}\phi^i\phi^j}} \quad (\text{B16})$$

makes Eq. (B12) into

$$f_{\mu\nu} = \bar{H}_f^{-2} \left[-f'^2(\phi^0)\partial_{\mu}\phi^0\partial_{\nu}\phi^0 + |K| \sinh^2 f(\phi^0) \Omega_{ij}^{(K)} \partial_{\mu}\phi^i\partial_{\nu}\phi^j \right], \quad (\text{B17})$$

which is of the form of Eq. (17) with $K < 0$ and $H_f = \bar{H}_f \coth f(\phi^0)$. The counterpart of Eq. (B9) is given by

$$X_{\pm} = \frac{\sqrt{|K|} \sinh(f(t))}{\bar{H}_f a(t)}. \quad (\text{B18})$$

Next, we consider the anti-de Sitter (AdS) fiducial metric given by

$$f_{\mu\nu} = - (1 + k^2 \delta_{ij} \varphi^i \varphi^j) \partial_\mu \varphi^0 \partial_\nu \varphi^0 + \Omega_{ij}^{(-k^2)} \partial_\mu \varphi^i \partial_\nu \varphi^j, \quad (\text{B19})$$

which is the AdS metric with curvature k in the global chart. Assuming $K < 0$, the field redefinition given by

$$\varphi^0 = k \arcsin \left(\frac{\sin f(\phi^0)}{\sqrt{1 - K \cos^2 f(\phi^0) \delta_{ij} \phi^i \phi^j}} \right), \quad \varphi^i = \frac{\sqrt{|K|}}{k} \cos f(\phi^0) \phi^i \quad (\text{B20})$$

make the fiducial metric into

$$f_{\mu\nu} = k^{-2} \left(-f'^2(\phi^0) \partial_\mu \phi^0 \partial_\nu \phi^0 + |K| \cos^2 f(\phi^0) \Omega_{ij}^{(K)} \partial_\mu \phi^i \partial_\nu \phi^j \right), \quad (\text{B21})$$

for which $H_f = k \tan f(\phi^0)$ and the counterpart of Eq. (B9) is

$$X_{\pm} = \frac{\sqrt{|K|} \cos f(t)}{k a(t)}. \quad (\text{B22})$$

We summarize these results in Table I. Note the the constraint equations, which are the counterparts of Eq. (B9), give restrictions on the trajectory of $a(t)$. For example, the constraint equation in the $K > 0$ case allows only the trajectory of $a(t)$ which starts from the infinity, decreases to the minimum and grows to the infinity again. Even though the $a(t)$ which starts from zero, increases to the maximum and comes back to zero is also allowed by the Friedmann equation, it is not consistent with the constraint equation and is not a cosmological solution in this model.

TABLE I: Results summary.

| | | φ^0 | φ^i | H_f | Constraint eq. |
|-----|---------|---|---|------------------------------|--|
| dS | $K > 0$ | $\bar{H}_f^{-1} \log \left[\sinh f(\phi^0) + \cosh f(\phi^0) \sqrt{1 - K \delta_{ij} \phi^i \phi^j} \right]$ | $\frac{\bar{H}_f^{-1} \sqrt{K} \phi^i}{\tanh f(\phi^0) + \sqrt{1 - K \delta_{ij} \phi^i \phi^j}}$ | $\bar{H}_f \tanh(f(\phi^0))$ | $X_{\pm} = \frac{\sqrt{K} \cosh f(t)}{\bar{H}_f a(t)}$ |
| | $K = 0$ | $f(\phi^0)$ | ϕ^i | \bar{H}_f | $X_{\pm} = \frac{\exp(\bar{H}_f f(t))}{a(t)}$ |
| | $K < 0$ | $\bar{H}_f^{-1} \log \left[\cosh f(\phi^0) + \sinh f(\phi^0) \sqrt{1 - K \delta_{ij} \phi^i \phi^j} \right]$ | $\frac{\bar{H}_f^{-1} \sqrt{ K } \phi^i}{\coth f(\phi^0) + \sqrt{1 - K \delta_{ij} \phi^i \phi^j}}$ | $\bar{H}_f \coth(f(\phi^0))$ | $X_{\pm} = \frac{\sqrt{ K } \sinh f(t)}{\bar{H}_f a(t)}$ |
| AdS | $K < 0$ | $k \arcsin \left(\frac{\sin f(\phi^0)}{\sqrt{1 - K \cos^2 f(\phi^0) \delta_{ij} \phi^i \phi^j}} \right)$ | $\frac{\sqrt{ K }}{k} \cos f(\phi^0) \phi^i$ | $k \tan f(\phi^0)$ | $X_{\pm} = \frac{\sqrt{ K } \cos f(t)}{k a(t)}$ |

Before closing this appendix, we briefly mention some examples of M_{GW} . For instance, in the case of the + blanch solution with the Minkowski fiducial metric,

$$M_{GW}^2|_{\text{Minkowski}} \propto (\dot{a} + \text{constant}). \quad (\text{B23})$$

As a result, $a^2 |M_{GW}^2|$ always grows with time, provided that the dominant fluid's equation of state is $w < 1$. Another example is the de Sitter fiducial metric, for which we have

$$M_{GW}^2|_{\text{deSitter}} \propto \left(\frac{\dot{a}}{a} + \text{constant} \right). \quad (\text{B24})$$

In this case, the contribution from the first term in $a^2 M_{GW}^2$ will grow if $w < 1/3$. Although for radiation dominated universe, this contribution is constant, the second term will still grow as a^2 . In the light of these examples and the late-time stability of the system, we adopt the assumption (25) throughout this paper.

Appendix C: Analytic solutions of γ_k

We show the analytic solution for Eq. (9) for power-law type $M_{GW}^2 = M_{\text{eq}}^2 (a/a_{\text{eq}})^p$, which covers the simple examples such as the constant M_{GW} and also the examples mentioned above. The aim of this section is to confirm the validity of the thin-horizon approximation used in Sec. IV.

We define the conformal time η from the scale factor $a = a_{\text{eq}}(t/t_{\text{eq}})^{1/2}$ (RD) and $a = a_{\text{eq}}(t/t_{\text{eq}})^{3/2}$ (MD) as

$$\eta \equiv \alpha \int_0^t \frac{dt}{a(t)} = \eta_{\text{eq}} \times \begin{cases} \frac{a}{a_{\text{eq}}} & \text{(RD)} \\ \frac{2}{3} \left(\frac{a}{a_{\text{eq}}} \right)^{1/2} - \frac{1}{2} & \text{(MD)} \end{cases} \Leftrightarrow \frac{a}{a_{\text{eq}}} = \begin{cases} \frac{\eta}{\eta_{\text{eq}}} & \text{(RD)} \\ \left(\frac{2}{3} \left(\frac{\eta}{\eta_{\text{eq}}} + \frac{1}{2} \right) \right)^2 & \text{(MD)} \end{cases}, \quad (\text{C1})$$

where α is a constant and $\eta_{\text{eq}} \equiv 2\alpha t_{\text{eq}}/a_{\text{eq}}$.

We consider the case that M_{GW} becomes dominant in the MD era first. Eq. (9) in this case becomes

$$\bar{\gamma}_k'' + \left(k^2 + a^2 M_{\text{eq}}^2 \left(\frac{a}{a_{\text{eq}}} \right)^p - \frac{a''}{a} \right) \bar{\gamma}_k = 0 \quad \Leftrightarrow \quad \frac{d^2 \bar{\gamma}_k}{d\hat{\eta}^2} + \left(\hat{k}^2 + \left(\frac{2}{3} \right)^{2(p+2)} \hat{M}_{\text{eq}}^2 \hat{\eta}^{2(p+2)} - \frac{2}{\hat{\eta}^2} \right) \bar{\gamma}_k = 0, \quad (\text{C2})$$

where we introduced $\hat{k} \equiv k\eta_{\text{eq}}$, $\hat{M}_{\text{eq}} \equiv a_{\text{eq}}\eta_{\text{eq}}M_{\text{eq}}$, $\hat{a} \equiv a/a_{\text{eq}}$ and $\hat{\eta} \equiv \frac{\eta}{\eta_{\text{eq}}} + \frac{1}{2} = 2\hat{a}^{1/2}/3$. Below, we use an approximation depending on which of k and aM_{GW} is dominant at the moment of the horizon crossing.

1. $k \gg aM_{GW}$ at the horizon crossing:

In this case, Eq. (C2) is approximated near the moment of the horizon crossing as

$$\frac{d^2 \bar{\gamma}_k}{d\hat{\eta}^2} + \left(\hat{k}^2 - \frac{2}{\hat{\eta}^2} \right) \bar{\gamma}_k = 0, \quad (\text{C3})$$

which is same as that in the pure GR. This equation has an exact solution which becomes regular for $\hat{k}\hat{\eta} \rightarrow 0$ given by

$$\bar{\gamma}_k = C \times \frac{3}{\hat{k}^2} \left(-\cos(\hat{k}\hat{\eta}) + \frac{\sin(\hat{k}\hat{\eta})}{\hat{k}\hat{\eta}} \right) \bar{\gamma}_k \xrightarrow{\hat{k}\hat{\eta} \ll 1} C\hat{\eta}^2. \quad (\text{C4})$$

The primordial amplitude is given by $|\gamma_k| = k^{-3/2}(H_*/M_{Pl})$ and

$$|\bar{\gamma}_k| = \frac{H_* a}{\hat{k}^{3/2} M_{Pl}} = \frac{4H_* a_{\text{eq}} \eta_{\text{eq}}^{3/2}}{9M_{Pl} \hat{k}^{3/2}} \hat{\eta}^2 \equiv \bar{\gamma}_* \hat{\eta}^2, \quad (\text{C5})$$

and then we may identify it with the right-hand side of Eq. (C4) in the limit of $\hat{k}\hat{\eta} \ll 1$. The solution in the WKB regime, on the other hand, is given by

$$\bar{\gamma}_k = \frac{C'}{\sqrt{\hat{k}}} \cos \left(\int \hat{k} d\hat{\eta} \right), \quad (\text{C6})$$

where $\hat{k}^2 \equiv (k^2 + a^2 M_{GW}^2) \eta_{\text{eq}}^2$. Comparing it with Eq. (C4) in the limit of $\hat{k}\hat{\eta} \gg 1$, we may fix the coefficient C' to have

$$\bar{\gamma}_k = \frac{3\bar{\gamma}_*}{\hat{k}^{3/2}} \cos \left(\int \hat{k} d\hat{\eta} \right). \quad (\text{C7})$$

Let us compare Eq. (C7) with γ_k obtained using the thin-horizon approximation. The condition to determine a at the horizon crossing is given by $k = a\dot{H} = a'/a = 2/\eta$. Matching the WKB solution with the primordial solution at η defined by this equation, we find the solution is given by

$$\bar{\gamma}_k = \frac{4\bar{\gamma}_*}{\hat{k}^{3/2}} \cos \left(\int \hat{k} d\hat{\eta} \right), \quad (\text{C8})$$

which coincide with Eq. (C7) up to a numerical factor.

2. $aM_{GW} \gg k$ at the horizon crossing:

Eq. (C2) in this case is approximated as

$$\bar{\gamma}_k'' + \left(a^2 M_{GW}^2 - \frac{a''}{a} \right) \bar{\gamma} = 0 \quad \Leftrightarrow \quad \frac{d\bar{\gamma}}{d\hat{\eta}^2} + \left(\left(\frac{2}{3} \right)^{2(p+2)} \hat{M}_{\text{eq}}^2 \hat{\eta}^{2(p+2)} - \frac{2}{\hat{\eta}^2} \right) \bar{\gamma}_k = 0, \quad (\text{C9})$$

which have an exact solution that becomes regular for $\hat{k}\hat{\eta} \rightarrow 0$ given by

$$\bar{\gamma}_k = C \times \frac{\left(\frac{3}{2} \right)^{\frac{3}{2}-\frac{3}{q}} q^{\frac{3}{q}} \Gamma\left(1 + \frac{3}{q}\right)}{\hat{M}_{\text{eq}}^{\frac{3}{q}}} \hat{\eta}^{1/2} J_{\frac{3}{q}} \left(\frac{3 \left(\frac{2}{3} \right)^{\frac{q}{2}} \hat{M}_{\text{eq}} \hat{\eta}^{\frac{q}{2}}}{q} \right) \xrightarrow{\hat{\eta} \rightarrow 0} C \hat{\eta}^2, \quad (\text{C10})$$

where J is the Bessel function and we have defined $q \equiv 2(p+3)$. Fixing C using Eq. (C5), we find $\bar{\gamma}_k$ to be

$$\begin{aligned} \bar{\gamma}_k = \bar{\gamma}_* \times \frac{\left(\frac{3}{2} \right)^{\frac{3}{2}-\frac{3}{q}} q^{\frac{3}{q}} \Gamma\left(1 + \frac{3}{q}\right)}{\hat{M}_{\text{eq}}^{\frac{3}{q}}} \hat{\eta}^{1/2} J_{\frac{3}{q}} \left(\frac{3 \left(\frac{2}{3} \right)^{\frac{q}{2}} \hat{M}_{\text{eq}} \hat{\eta}^{\frac{q}{2}}}{q} \right) \\ \xrightarrow{\hat{\eta} \rightarrow \infty} \frac{q^{\frac{3}{q}+\frac{1}{2}} \Gamma\left(1 + \frac{3}{q}\right)}{\sqrt{\pi}} \times \frac{\bar{\gamma}_* \left(\frac{3}{2} \right)^{\frac{3}{2}-\frac{3}{q}} \hat{M}_{\text{eq}}^{-\frac{3}{q}}}{\sqrt{\left(\frac{2}{3} \right)^{\frac{q}{2}-1} \hat{M}_{\text{eq}} \hat{\eta}^{\frac{q}{2}-1}}} \cos \left(\frac{3 \left(\frac{2}{3} \right)^{\frac{q}{2}} \hat{M}_{\text{eq}} \hat{\eta}^{\frac{q}{2}}}{q} \right), \quad (\text{C11}) \end{aligned}$$

where we neglected the phase of the oscillation. This expression is valid as long as M_{GW} dominates over k/a . Below, we compare it with the expression obtained from the thin-horizon approximation. The condition to determine η at the horizon crossing is given by

$$\left(\frac{2}{3} \right)^{2(p+2)} \hat{M}_{\text{eq}}^2 \hat{\eta}^{2(p+2)} = \frac{2}{\hat{\eta}^2} \quad \therefore \quad \eta = 2^{\frac{1}{2(p+3)}} \left(\frac{3}{2} \right)^{\frac{p+2}{p+3}} \hat{M}_{\text{eq}}^{-\frac{1}{p+3}}. \quad (\text{C12})$$

Matching the WKB solution with the primordial solution at this η , we find

$$\bar{\gamma}_k = 2^{\frac{1}{4}+\frac{3}{2q}} \times \frac{\bar{\gamma}_* \left(\frac{3}{2} \right)^{\frac{3}{2}-\frac{3}{q}} \hat{M}_{\text{eq}}^{-\frac{3}{q}}}{\sqrt{\hat{k}}} \cos \left(\int \hat{k} d\hat{\eta} \right). \quad (\text{C13})$$

This expression coincides with Eq. (C11) up to an $\mathcal{O}(1)$ factor for generic $q > 0$, and thus the thin-horizon approximation is fairly good even in this case.

Finally, we briefly comment on the case that M_{GW} becomes dominant in the RD era. In this case, Eq. (9) becomes $\bar{\gamma}'' + (k^2 + a^2 M_{GW}^2) \bar{\gamma} = 0$. As long as $k^2 + a^2 M_{GW}^2$ is positive and its time variation is sufficiently slow, the solution will be well approximated by the WKB solution. The amplitude of this solution is determined by matching it to the primordial solution. By construction, this solution will be well approximated by the solution given by the thin-horizon approximation in general.

-
- [1] M. Fierz and W. Pauli, Proc. Roy. Soc. Lond. A **173**, 211 (1939).
 - [2] D. G. Boulware, S. Deser, Phys. Rev. **D6**, 3368-3382 (1972).
 - [3] C. de Rham, G. Gabadadze, Phys. Rev. **D82**, 044020 (2010). [arXiv:1007.0443 [hep-th]].
 - [4] C. de Rham, G. Gabadadze, A. J. Tolley, Phys. Rev. Lett. **106**, 231101 (2011). [arXiv:1011.1232 [hep-th]].
 - [5] S. F. Hassan, R. A. Rosen, [arXiv:1106.3344 [hep-th]].
 - [6] C. de Rham, G. Gabadadze, A. Tolley, [arXiv:1107.3820 [hep-th]].
 - [7] C. de Rham, G. Gabadadze, A. J. Tolley, [arXiv:1108.4521 [hep-th]].
 - [8] S. F. Hassan, R. A. Rosen, A. Schmidt-May, [arXiv:1109.3230 [hep-th]].
 - [9] S. F. Hassan and R. A. Rosen, JHEP **1204**, 123 (2012) [arXiv:1111.2070 [hep-th]].
 - [10] M. Mirbabayi, arXiv:1112.1435 [hep-th].
 - [11] A. Golovnev, Phys. Lett. B **707**, 404 (2012) [arXiv:1112.2134 [gr-qc]].
 - [12] C. de Rham, G. Gabadadze, L. Heisenberg, D. Pirtskhalava, Phys. Rev. **D83**, 103516 (2011). [arXiv:1010.1780 [hep-th]].

- [13] K. Koyama, G. Niz, G. Tasinato, Phys. Rev. Lett. **107**, 131101 (2011). [arXiv:1103.4708 [hep-th]].
- [14] T. M. Nieuwenhuizen, Phys. Rev. **D84**, 024038 (2011). [arXiv:1103.5912 [gr-qc]].
- [15] K. Koyama, G. Niz, G. Tasinato, Phys. Rev. **D84**, 064033 (2011). [arXiv:1104.2143 [hep-th]].
- [16] A. H. Chamseddine, M. S. Volkov, Phys. Lett. **B704**, 652-654 (2011). [arXiv:1107.5504 [hep-th]].
- [17] G. D'Amico, C. de Rham, S. Dubovsky, G. Gabadadze, D. Pirtskhalava and A. J. Tolley, Phys. Rev. D **84**, 124046 (2011) [arXiv:1108.5231 [hep-th]].
- [18] A. E. Gumrukcuoglu, C. Lin and S. Mukohyama, JCAP **1111**, 030 (2011) [arXiv:1109.3845 [hep-th]].
- [19] K. Koyama, G. Niz and G. Tasinato, JHEP **1112**, 065 (2011) [arXiv:1110.2618 [hep-th]].
- [20] D. Comelli, M. Crisostomi, F. Nesti and L. Pilo, Phys. Rev. D **85**, 024044 (2012) [arXiv:1110.4967 [hep-th]].
- [21] M. S. Volkov, JHEP **1201**, 035 (2012) [arXiv:1110.6153 [hep-th]].
- [22] M. von Strauss, A. Schmidt-May, J. Enander, E. Mortsell and S. F. Hassan, JCAP **1203**, 042 (2012) [arXiv:1111.1655 [gr-qc]].
- [23] D. Comelli, M. Crisostomi, F. Nesti and L. Pilo, JHEP **1203**, 067 (2012) [arXiv:1111.1983 [hep-th]].
- [24] L. Berezhiani, G. Chkareuli, C. de Rham, G. Gabadadze and A. J. Tolley, Phys. Rev. D **85**, 044024 (2012) [arXiv:1111.3613 [hep-th]].
- [25] Y. Brihaye and Y. Verbin, arXiv:1112.1901 [gr-qc].
- [26] T. Kobayashi, M. Siino, M. Yamaguchi and D. Yoshida, arXiv:1205.4938 [hep-th].
- [27] N. Arkani-Hamed, H. -C. Cheng, M. A. Luty and S. Mukohyama, JHEP **0405**, 074 (2004) [hep-th/0312099].
- [28] N. Arkani-Hamed, H. -C. Cheng, M. A. Luty, S. Mukohyama and T. Wiseman, JHEP **0701**, 036 (2007) [hep-ph/0507120].
- [29] V. A. Rubakov, hep-th/0407104.
- [30] S. L. Dubovsky, JHEP **0410**, 076 (2004) [hep-th/0409124].
- [31] A. De Felice, A. E. Gumrukcuoglu and S. Mukohyama, arXiv:1206.2080 [hep-th].
- [32] G. D'Amico, arXiv:1206.3617 [hep-th].
- [33] A. E. Gumrukcuoglu, C. Lin and S. Mukohyama, JCAP **1203**, 006 (2012) [arXiv:1111.4107 [hep-th]].
- [34] D. Langlois and A. Naruko, arXiv:1206.6810 [hep-th].
- [35] C. de Rham and S. Renaux-Petel, arXiv:1206.3482 [hep-th].
- [36] A. E. Gumrukcuoglu, C. Lin and S. Mukohyama, arXiv:1206.2723 [hep-th].
- [37] G. D. Moore and A. E. Nelson, JHEP **0109**, 023 (2001) [hep-ph/0106220].
- [38] R. Kimura and K. Yamamoto, JCAP **1207**, 050 (2012) [arXiv:1112.4284 [astro-ph.CO]].
- [39] G. W. Horndeski, Int. J. Theor. Phys. **10** (1974) 363-384.
- [40] T. Kobayashi, M. Yamaguchi and J. 'i. Yokoyama, Prog. Theor. Phys. **126**, 511 (2011) [arXiv:1105.5723 [hep-th]].
- [41] K. Danzmann, Class. Quant. Grav. **14**, 1399 (1997).
- [42] N. Seto, S. Kawamura and T. Nakamura, Phys. Rev. Lett. **87**, 221103 (2001).
- [43] A. R. Taylor, A. R. 2008, IAU Symposium, 248, 164
- [44] G. B. Hobbs, M. Bailes, N. D. R. Bhat, S. Burke-Spolaor, D. J. Champion, W. Coles, A. Hotan and F. Jenet *et al.*, arXiv:0812.2721 [astro-ph].
- [45] T. Clifton, P. G. Ferreira, A. Padilla and C. Skordis, Phys. Rept. **513**, 1 (2012) [arXiv:1106.2476 [astro-ph.CO]].
- [46] C. de Rham, A. J. Tolley and D. H. Wesley, arXiv:1208.0580 [gr-qc].
- [47] E. Komatsu *et al.* [WMAP Collaboration], Astrophys. J. Suppl. **192**, 18 (2011) [arXiv:1001.4538 [astro-ph.CO]].
- [48] A. Sesana and A. Vecchio, Class. Quant. Grav. **27**, 084016 (2010) [arXiv:1001.3161 [astro-ph.CO]].
- [49] P. Amaro-Seoane, S. Aoudia, S. Babak, P. Binetruy, E. Berti, A. Bohe, C. Caprini and M. Colpi *et al.*, arXiv:1201.3621 [astro-ph.CO].
- [50] <http://www.ligo.caltech.edu/>
- [51] <http://gwcenter.icrr.u-tokyo.ac.jp/en/>
- [52] F. A. Jenet, G. B. Hobbs, K. J. Lee and R. N. Manchester, Astrophys. J. **625**, L123 (2005) [astro-ph/0504458].
- [53] S. Dubovsky, R. Flauger, A. Starobinsky and I. Tkachev, Phys. Rev. D **81**, 023523 (2010) [arXiv:0907.1658 [astro-ph.CO]].
- [54] C. M. Will, Phys. Rev. D **57**, 2061 (1998) [gr-qc/9709011].
- [55] M. Maggiore, Phys. Rept. **331**, 283 (2000) [gr-qc/9909001].
- [56] M. Fasiello and A. J. Tolley, arXiv:1206.3852 [hep-th].